A METHODOLOGY FOR GRASP ROBUSTNESS UNDER SHAPE UNCERTAINTY

By
ATUL GUPTA

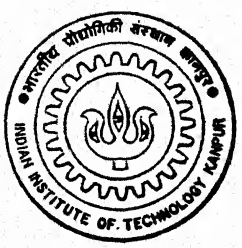

DEPARTMENT OF MECHANICAL ENGINEERING
Indian Institute of Technology Kanpur

NOVEMBER 1997

A METHODOLOGY FOR GRASP ROBUSTNESS UNDER SHAPE UNCERTAINTY

A Thesis Submitted

in Partial Fulfilment of the Requirements

for the Degree of

Master of Technology

by

ATUL GUPTA

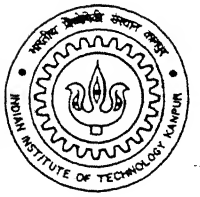

to the

DEPARTMENT OF MECHANICAL ENGINEERING

INDIAN INSTITUTE OF TECHNOLOGY KANPUR

November, 1997

1E-1997-M-GUP-MET

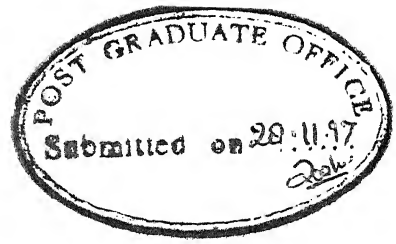

CERTIFICATE

It is certified that the work contained in the thesis entitled **A METHODOLOGY FOR GRASP ROBUSTNESS UNDER SHAPE UNCERTAINTY** by Mr. **Atul Gupta**, has been carried out under my supervision and that this work has not been submitted elsewhere for a degree.

Dr. A. Mukerjee
Associate Professor
Department of Mechanical Engineering
Indian Institute of Technology Kanpur
Kanpur, 208016

November, 1997

Dedicated to -

My Parents

Acknowledgements

With immense pleasure I express my indebtedness and a deep sense of gratitude to Dr. A. Mukerjee, whose guidance and encouragement at every step through constructive criticisms and fruitful suggestions helped me through the successful completion of this work. He has been a great influence on me, both, as a person and as a professional.

I am thankful to Prof. H. Hatwal for extending the facilities of the Center for Robotics for the completion of this work. It was a pleasure to be associated with Center for Robotics and I would like to thank all my colleagues and staff at Center for Robotics for making it a great place to work in.

Above all, I am blessed with such caring parents. I extend my deepest gratitude to my parents for their invaluable love, affection, encouragement and support. Thanks to my sister Anshu for her constant inspiration in my effort to do this work.

I would like to thank my friends Vikas Saxena, Brijesh Singh, Sambit Dash, Suman, Satya Parkash and Sudhir for their warm affections to make my stay at IIT Kanpur a pleasant one.

Last but not the least I would like to express my gratefulness to all those who directly or indirectly helped me through the successful completion of my work.

Atul Gupta
IIT Kanpur
November, 1997

Abstract

For synthesizing grasps, one needs to know the shape of the object. Shapes are often uncertain due to errors in geometric model, sensors etc. Furthermore, the nature of contact friction is uncertain and often unknown. Given a planar polygonal shape, a nominal grasp strategy can be obtained. But how well will this work under uncertainty? Given a shape with known uncertainty, how robust is the nominal grasp based on the nominal shape of the polygon? We show that analytical methods can only provide an incomplete answer to this question and in this work we attempt to provide a methodology for assessing this empirically.

Defining a polygon class of uncertain polygons for known uncertainty, large sets of polygons are generated from this class to find the robustness of a grasp, computed on the basis of the nominal polygon geometry. Uncertainties in the shape of the polygon are modeled in two types:

- Vertex Position Uncertainty Model: The vertex based model ,where position of the vertices of the object are uncertain.
- Edge Length/Orientation Uncertainty Model: Where as the edge based model deals where length of edges and angles between adjacent edges of the object are uncertain.

The main contribution of this work is to develop a model for handling shape uncertainty and an empirical methodology for finding robustness of grasps under shape uncertainty. This is done by generating a sufficiently large number of polygons from the uncertain polygon class. A secondary contribution may be in development of random polygon generator.

Contents

List of Figures

Chapter 1

Introduction

1.1 Description

A key problem in robot manipulation is the presence of uncertainty. Uncertainty arises both in the robot's knowledge of the surrounding world and in its ability to execute motions. The presence of uncertainty in a task environment can lead to unpredictable, perhaps, undesirable results. The first step in a proper manipulation of an object is a stable grasp and for synthesising grasps, one needs to know the shape of the object. Shapes are often uncertain due to errors in the geometric models, sensors, etc. Due to these, grasp synthesis based on a nominal model of the shape may not work on the actual part. It is important to determine the extent to which a given grasp can handle shape uncertainty, this may be called the *robustness* of the given grasp.

This question has been addressed at different levels such as object positioning errors [4], cumulative force/position errors [3] and errors in parallel jaw grasping [1], but the specific aspect of shape uncertainty has not been looked at. The robustness of a grasp depends critically on the shape of the part being grasped, for example higher uncertainties can be tolerated in parts with longer aspect ratios (Figure 3.14). Thus it is important to be able to model the effects arising from shape uncertainty in the specific part being grasped. Some models such as generalized cones [7] consider grasping for model uncertainty in the very limited sense of axially, symmetric shapes.

To a large part the inability to handle shape uncertainty is due to a poverty of CAD itself, which has largely remained focused on "Unambiguous" models [12], i.e. models which have a single, exact instantiation. Thus shape variations simply can not be modeled. Creating such models is one of the main contributions of this work.

Here we develop two general purpose shape ambiguity models, and then focuses on this critical question: Given an object to be grasped and the nature of the modeling/sensing/positioning uncertainties, what should be the methodology in order to obtain an estimate of the grasp robustness?

There are a number of shape uncertainty models available, such as topological [2], spatial occupancy models [8], medial axis or skeleton models [9], vertex visibility models [13], chain code models [6] etc. The problem here is that it is not clear how one should model the uncertainty that arises due to shape errors. Shape model data is often specified in terms of vertex position and model errors are reflected in terms of the *Vertex Position Uncertainty*. Sensor data from visual/tactile sensors often provide edge data, and therefore the errors are reflected in *Edge Length/Orientation Uncertainty*. Considering this, for the class of planar polygonal objects, we model shape uncertainty in two ways:

- *Vertex Uncertainty* : The vertices of the polygon have some position uncertainty, e.g. due to modeling inaccuracies (Figure 1.1).
- *Edge Uncertainty* : Here the polygon is modeled as a set of edge lengths and the angles between edges(chain-code). This information may be uncertain, e.g. edge-length may be uncertain in visual sensing (Figure 1.2).

Our approach is based on empirical data, similar to Monte Carlo Simulation. We use the well-known Van-Duc Nguyen algorithm [10] for finding a nominal force-closure grasp on the nominal polygon. For both of these shape uncertainty models, we generate a sufficiently large set of polygons from the uncertain polygon class, and determine the percentage of polygons in each set which can be grasped in a stable manner using the nominal grasp. This is our measure of grasp robustness.

Where the part information is uncertain mostly in the edge-length, our results indi-

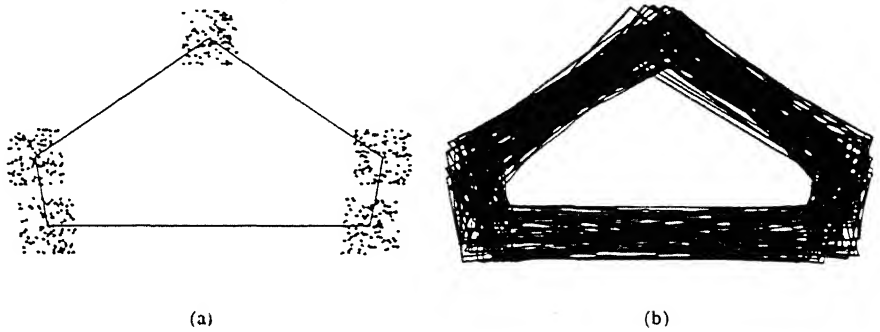

Figure 1.1: *Vertex Uncertainty.* Possible shapes under vertex uncertainty. If the vertex information is correct within 35% of the minimum edge length, then for the input data as in Figure. actual shape may be any of the above. (a) Nominal Polygon and Scatterd points within the vertex uncertainty bound. (b) Cluster of 100 such polygons.

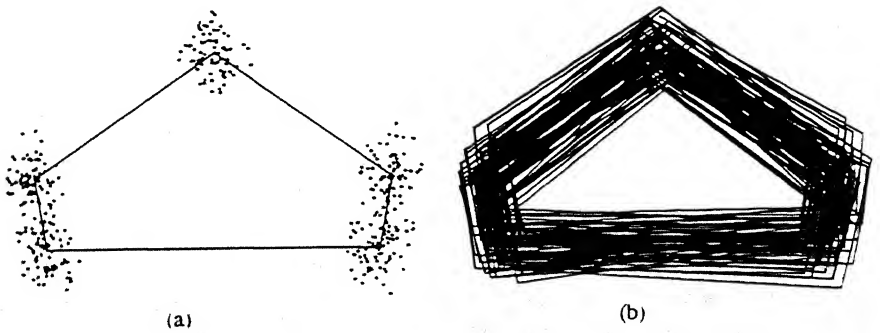

Figure 1.2: *Edge Uncertainty.* Possible shapes under edge uncertainty. If the adjacent edge angle information is correct within 3.6° and edge length within 35% of the minimum edge length, therefor the input shape as shown, actual shape may be any of the above. (a) Nominal Polygon and Scatterd points within the edge uncertainty bound. (b) Cluster of 100 such polygons.

cate relatively high robustness than in models where the vertex positions or edge-angles have errors. In practice, edge angle uncertainty is often small, except for very short edges, whereas sensing errors in edge length is quite common. In general lower uncertainty levels and higher coefficients of friction result in higher grasp robustness. However, it is the specific shape of the part which mainly affects the robustness. For initially infeasible grasps, an anomalous case is observed: as the model uncertainty increases the percentage of successful grasp may increase, since some of the perturbed shapes now provide a valid grasp.

1.2 Setup

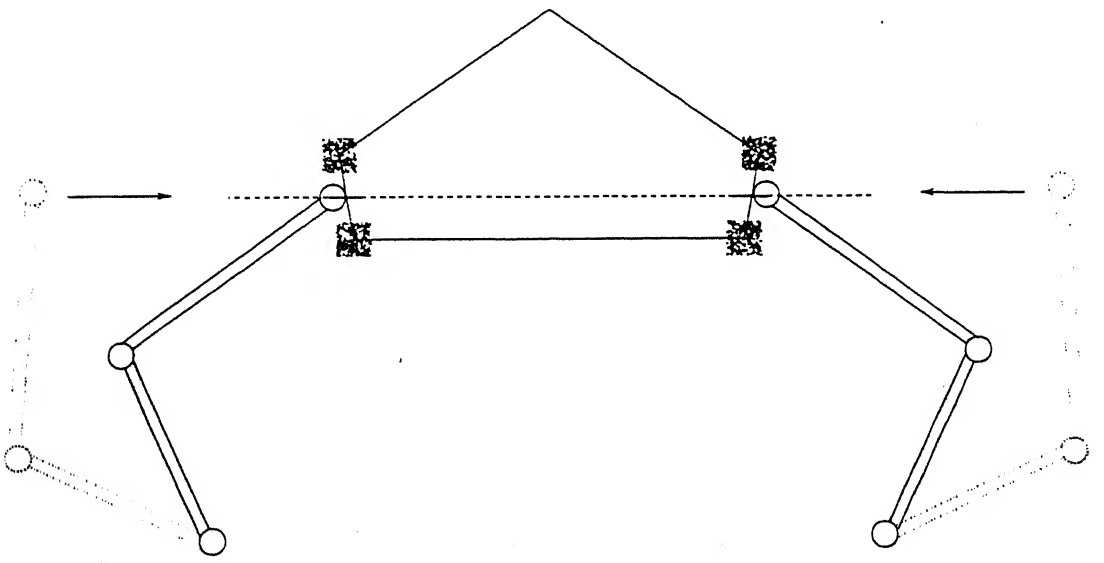

Figure 1.3: *The Robot hand.* Two 2-DOF fingers are used to grasp a planar polygonal object whose edges are uncertain. The fingertips move to the nominal grasp points along the direction of the line joining them. Scatter-plots show the vertex position uncertainty on each of the contact edges (10% of the smallest edge length. 700 of 1000 polygons are graspable with the nominal grasp.

Figure 1.3 shows the schematic setup for planar two-finger grasping. Given the exact shape of the object to be grasped, it is known that force-closure can be obtained for planar friction grasps with two point contacts. As the fingertips move to the nominal grasp points along the grasp trajectory. With shape uncertainty, they will

contact the edges at some point other than the nominal contact. The resulting grasp may not be a force closure

The objective of this work is to develop a methodology for finding robustness of grasps under shape uncertainty. This uncertainty may arise due to errors in the model of the object, position or orientation error. This work does not address other sources of error such as robot self-position error, finger geometry error etc.

1.3 Assumptions and Frame work

In order to find the grasp points on the nominal polygon we have used Nguyen's algorithm [10] which is a fast, well known algorithm for planar grasp synthesis. It is not directed towards any particular task, so task-dependent aspects are not important. The basic approach, using force-closure, is common to all grasping solutions. Moreover, also due to uncertainty in grasping points we have used this algorithm, because it gives the range of grasping points in terms of IROCs(defined later) instead of one discrete grasping point for each finger.

Given a nominal polygonal shape and a bound on the degree of uncertainty, the shape class corresponding to this uncertainty can be defined. The grasp system however is not aware of the actual object geometry, and proceeds to grasp it at two nominal points identified as optimal by the force-closure algorithm. The direction of approach of the finger is assumed to be the line joining the nominal grasp points (Figure 1.3).

This thesis describes a methodology for assessing robustness of 2D grasp based on errors in the information of shape. Chapter 2 explains the synthesis of the nominal grasp by Van-Duc Nguyen algorithm. Chapter 3 explains the two uncertainty models and the methodology for estimating the robustness of the nominal grasp. Along this a possible analytical approach for assessing the grasp robustness for some type of grasp failure is discussed in Chapter 3. We also discuss the tests on different polygons and summarize the results . Chapter 4 discuss the ramification of this work and possible extensions.

Chapter 2

Graspability and Shape Uncertainty

2.1 Grasp and Graspability

Grasping of planar objects have been analyzed widely by ([5], [10],[11]) a number of other researchers. A planar object grasped by j fingers, each exerting force $\mathbf{f_j}$ at respective contact points, should satisfy two necessary conditions for a stable grasp. First, the object must be in equilibrium i.e the net external force and moment must be balanced by the contact forces.

$$\sum \mathbf{f_j} = \mathbf{F} \tag{2.1}$$

$$\sum \mathbf{r_j} \times \mathbf{f_j} = \mathbf{M} \tag{2.2}$$

where $\mathbf{f_j}$ are the j force vectors and $\mathbf{r_j}$ are the distance vectors from a fixed point to the contact point on each finger. $\mathbf{F}$ and $\mathbf{M}$ are the net external force and moment on the object.

Secondly, for no slip at the fingers, all forces must lie within the cone of friction as in Figure 2.1. The contact forces have surface normal components, $\mathbf{f_n}$ and tangent

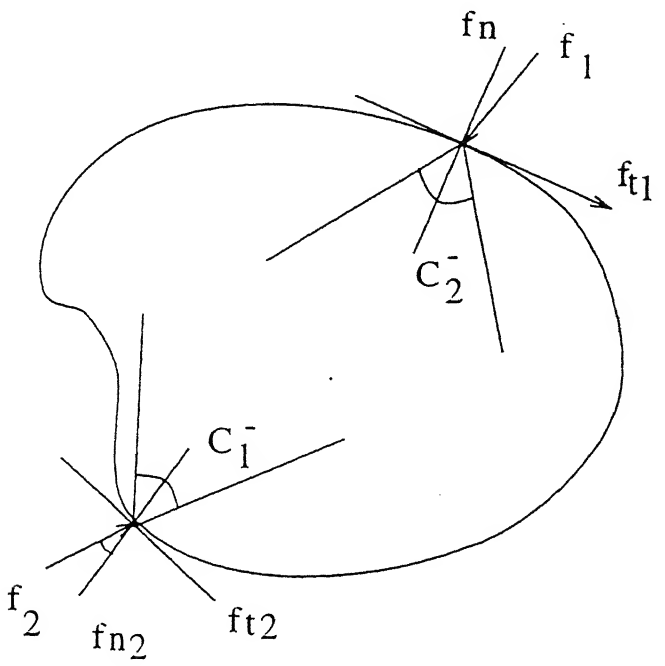

Figure 2.1: *Planar Object Grasp Forces:* C_1^- and C_2^- are the friction cones for squeezing grasp.

component f_t. The relative magnitudes of these forces are governed by the coulomb inequality.

$$| f_t | \leq \mu | f_t | \tag{2.3}$$

Where μ is the coefficient of static friction at the contact point. Therefore the angle α_j that the contact force can make with the normal is subjected to the constraint

$$| \alpha_j | \leq tan^{-1} \mu = \phi \tag{2.4}$$

Where ϕ is the friction angle.

For the condition of graspability, consider the portion of a polygon grasped by two fingers as in Figure 2.2. If no external forces or moments are acting on the polygon, for equilibrium, the two forces must be collinear, of equal magnitude and opposite sign. Therefore, for a polygon, the two force angles cannot be independent, and are

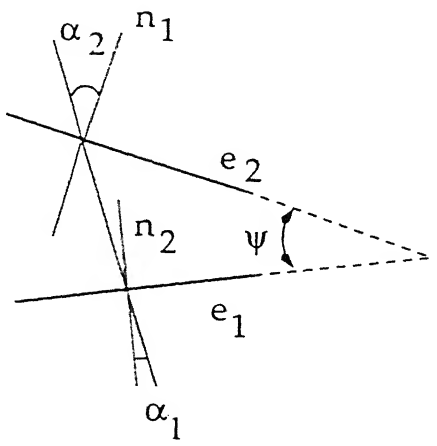

Figure 2.2: Graspability for Given Two Edges

related by

$$\alpha_2 = \alpha_1 + \psi \tag{2.5}$$

Where ψ is the angle between the surface normals (or in other words the angle between the edges on which the fingers are placed). Thus for stable grasp of a polygon

$$| \psi | < 2 | \phi | \tag{2.6}$$

The closer the sides are to being parallel, the smaller the coefficient of friction is required to grasp them stably.

2.2 Force-Closure grasp of Planar Objects

A grasp on an object is a force-closure grasp if and only if we can exert, through the set of contacts, arbitrary forces and moments on this object. Equivalently, any motion of the object can be resisted by a contact force, which means that the object cannot break contact with the fingers without some non-zero external work.

The forward grasp planning problem is to find places to put the fingertips, such that the grasp is force-closure. The reverse problem is to analyze whether a grasp, defined by a set of contacts, is force-closure or not. The reverse problem is one of practical importance in determining the grasp points. Furthermore, due to uncertainties in sensing and grasp execution, it is desirable to have a margin of error in selecting the grasp. The approach adopted formalizes this notion in terms of determining two independent regions of contact (**IROC**) [10].

Independent Regions of Contact (IROCs): For a gripper with k fingers independent regions of contacts are k regions on the graspable surfaces, such that so long as each finger is placed within its region, the grasp is force-closure and stable.

In this work, we investigate planar grasps where two contacts suffice (k=2). Grasped objects are arbitrary polygons. The contacts between the fingertips and the grasped object are modeled as point contacts with friction (Figure 2.3). shows example of force-closure grasps of planar objects. The independent regions of contact for the fingertips are highlighted by bold segments. Either contact can be placed anywhere within these regions and yet result in a force- closure grasp.

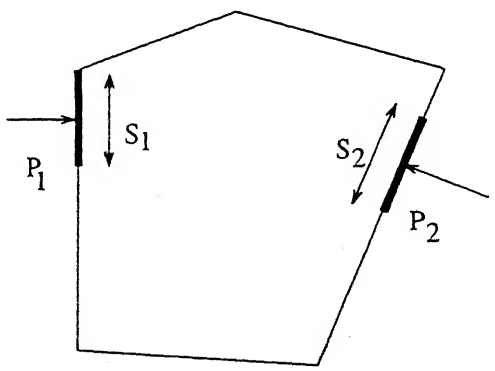

Figure 2.3: Grasping using Nguyen's Algorithm. $\mathbf{P_1}$ and $\mathbf{P_2}$ are the contact points and $\mathbf{S_1}$ and $\mathbf{S_2}$ are the IROCs on the respective edges. $\mathbf{P_1}$ can be positioned anywhere along $\mathbf{S_1}$ and $\mathbf{P_2}$ along $\mathbf{S_2}$ and the grasp remains stable.

2.2.1 Two Finger Grasp

For grasping using two fingers with friction, the line $\mathbf{P_1P_2}$ joining the contact points $\mathbf{P_1}$ and $\mathbf{P_2}$ on the object surface must lie within the friction cones $\mathbf{C_1^{\leqslant}}$ and $\mathbf{C_2^{\leqslant}}$

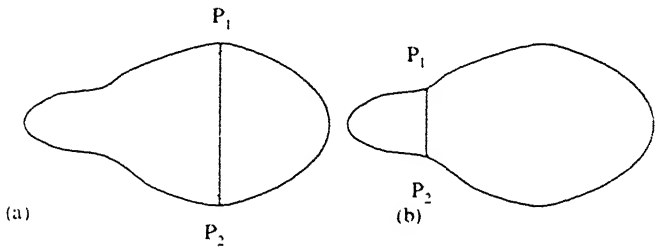

Figure 2.4: (a) A stable grasp, as the line joining the contact points is in the friction cones of both edges. (b) An unstable grasp as the line joining the contact points is out of friction cones.

respectively as shown in Figure 2.5.

A friction cone C_j, at contact point P_j consists of two sectors. the positive friction cone C_j^+ extending outside the object and the negative friction cone C_j^- extending inside the object (Figure 2.5 and 2.6). Both squeezing grasps where segment P_1P_2 falls inside C_1^- and C_2^-, and expanding grasps where segment P_1P_2 lies in C_1^+ and C_2^+ may satisfy force-closure conditions. A convex object can be grasped by squeezing grasps only. Non-convex objects may admit both squeezing and expanding grasps.

Given two friction cones C_1^- and C_2^-, we define the counter-overlapping sector $C^< = C_1^- \cap -C_2^-$; and for any two given points P_1 and P_2 the grasp is force-closure stable if and only if $C^<$ is not null as shown in Figure 2.5 and 2.6.

2.2.2 Finding the IROC on Two Edges

Finding independent regions of contact on two edges, is equivalent to positioning a two-sided cone ($\pm C^<$) such that its intercepts on these two edges are not null (Figure 2.7). These intercepts are the two IROCs. One objective of finding the IROC is to have a grasp such that the fingers can be positioned independently from each other, not at discrete points, but within large regions of the edges. Any two contacts over these segments will result in P_1P_2 lying inside $C^<$ and will therefore be a stable force closure grasp.

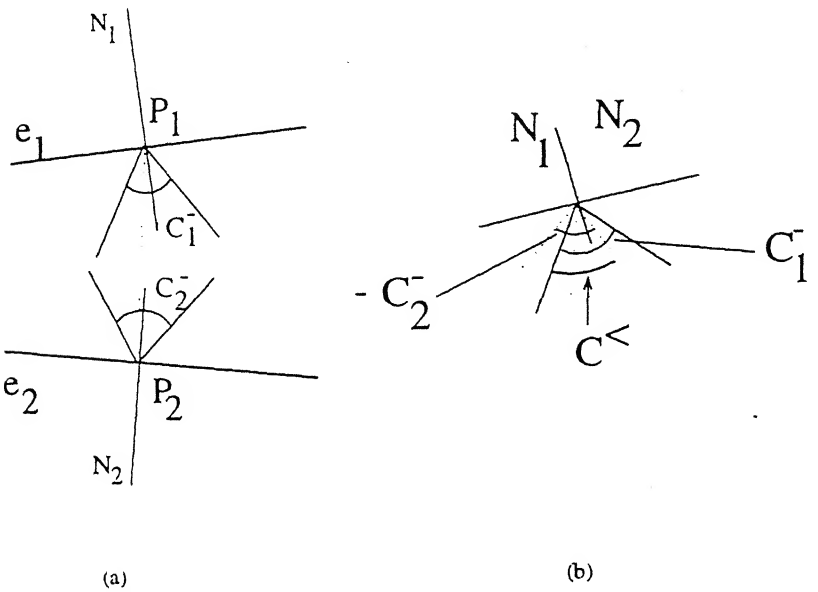

Figure 2.5: (a) Squeezing Grasp for a polygonal object on its two edges $\mathbf{e}_1$ and $\mathbf{e}_2$, N_1 and N_2 are the two normals at contact points $\mathbf{P}_1$ and $\mathbf{P}_2$. (b) As both normals are in their respective friction cones and the line joining the contact point is in the common region ($\mathbf{C}^<$) of the two friction cones it is a stable grasp.

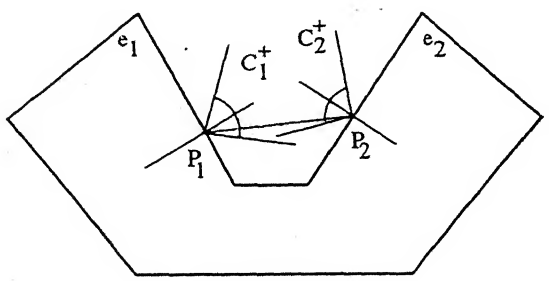

Figure 2.6: A stable expanding grasp for a Non Convex Polygonal Object

Algorithm for Finding IROC The following algorithm is based on Van-Duc Nguyen([10],[11]) algorithm.

- Position the cone $C^<$ with vertex I_1 such that it cuts all of the edge e_1 and very little or none of edge e_2. We get a triangle Δ_1 formed by edge e_1 and vertex I_1.
- Similarly we position the cone $C^<$ with vertex I_2 such that this later cuts exactly the edge e_2 and very little or none of edge e_1. We get a triangle Δ_2 formed by edge e_2 and vertex I_2.
- Find the trade-off region (χ) by intersecting the triangle Δ_1 with Δ_2. This region is the locus of vertex I, for which a two-sided cone $(I, \pm C^<)$ cuts both edges e_1 and e_2 into IROC segments S_1 and S_2. The lengths of the IROC segments is proportional to the distance of I from the respective edges.
- Equalize the two IROCs by choosing I to lie on the bisector of the edges e_1 and e_2. If the edges are not parallel, the optimal vertex I^* is at one of the two end points of the intercept of the bisector on region χ shown in Figure 2.7.
- From the optimal vertex, the independent regions of contact S_1 and S_2 are found by intercepting the two-sided cone $C^\times(I^*, \pm C^<)$ on the grasping edges e_1 and e_2.

2.2.3 Grasp Synthesis for Planar Polygonal Objects

We now proceed to determine the grasp points on a polygonal shape such that frictional contact at these points will be force-closure and provide some margin for placement error.

- Determine the friction cone angle ϕ for given value of the friction coefficient μ ($\phi = tan^{-1}\mu$).
- For each pair of edges, check that the edge angle $\psi < 2\,\phi$.

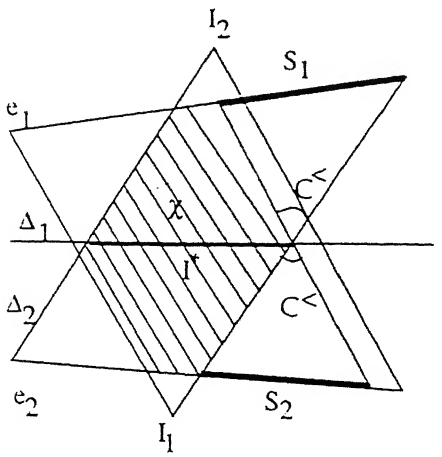

Figure 2.7: *Determination of IROCs.* By placing the apex of a double cone $C^{\times}$ ($I^* : \pm C^{<}$) on the bisect of two edges, the intercepts are guaranteed to be IROCs. This is maximal toward the divergent end.

- Find the IROC for those pairs which satisfy the above condition. This may be done by projecting a double cone from the bisector of the two edges as in Figure 2.7.
- Choose the pair of edges having maximum length of IROC.
- Mid points of the IROC lengths give the grasping points.

This algorithm, in its worst case, can have $\begin{pmatrix} n \\ 2 \end{pmatrix}$ edge pairs, and therefore runs in $O(n^2)$ time.

2.2.4 Grasp Trajectory

Having identified a nominal grasp which is force-closure and also permits some degree of placement uncertainty, we now need to determine a grasp trajectory along which robot fingers will approach to the object. There may be many choices, but the two main choices are either normal to each edge or along the line joining the two contact points. We are using the line joining the two contact points in finding the robustness of the nominal grasp, however any feasible direction for robot fingers to grasp the object can be used.

In the following chapter, we seek an answer to the question: Given a nominal grasp and grasp trajectory, how can we determine its robustness against variation in the object shape. Two analyze this, it is first necessary to investigate the types of shape variations that may arise. This is modeled in the following chapter.

Chapter 3

Modeling Shape Uncertainty and Assessing Grasp Robustness

This chapter presents the two original contributions of this work *a model for handling uncertain shapes* (Section 3.1) and *a methodology for finding robustness of the nominal grasp* (Section 3.4) and the empirical results are presented in Section 3.5.

3.1 Shape Uncertainty

Shape uncertainty is modeled using two approaches.

- *Vertex Position Uncertainty* : Where position of the vertices of the object are uncertain.
- *Edge Length/Orientation Uncertainty* : Where length of edges and angles between adjacent edges of the object are uncertain.

Geometric models usually define the vertices, so the vertex uncertainty model is more appropriate for uncertainty related to the task knowledge base.

Visual sensors are often more robust in detecting edges than vertices, so the Edge Uncertainty or chain-code model is more appropriate for situations where the object shape is being obtained visually.

3.1.1 Vertex Position Uncertainty

Here the polygon is represented as an ordered list of vertices. Hence the shape uncertainty results in a range of values for each vertex coordinates. In reconstructing the polygon a random value is chosen from this range for each vertex and these are connected, as in Figure 3.2. In some cases, the contour may self intersect, and these are infeasible polygons and are pruned from the data set.

3.1.2 Edge Length/Orientation Uncertainty

Here the polygon is represented as chain of edges with given edge length and and angle. The angle is relative to the previous edge. This model is also called the chain code model, and has the problem that the last edge may not close the polygon due to numerical error or data inaccuracy. In this model the shape uncertainty results in a range of values for each edge length and the angle between two adjacent edges. Which results in a region similar to Figure 3.1 in which the second vertex will lie, with respect to first vertex of a chain code model. Similarly for each point there will be such a region with respect to the previous point (which will also lie in some such uncertain region) of the chain code.

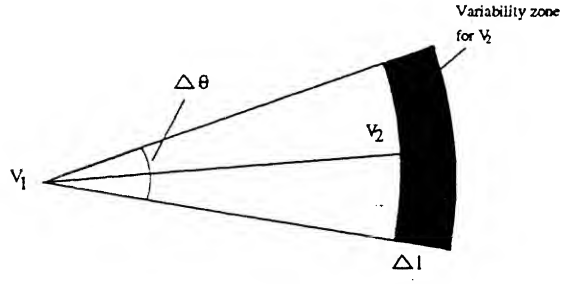

Figure 3.1: *Edge Length/Orientation Uncertainty.* The shaded region represents the range for the Vetex V_2, because of uncertainty Δl in edge length and angle uncertainty $\Delta\theta$ in the orientation of edge V_1V_2.

3.2 Effect of Shape Uncertainty on Grasping

When a robot's fingers try to grasp an object at two points of nominal grasp, because of the uncertainty in the shape of the object, the actual contact points may vary

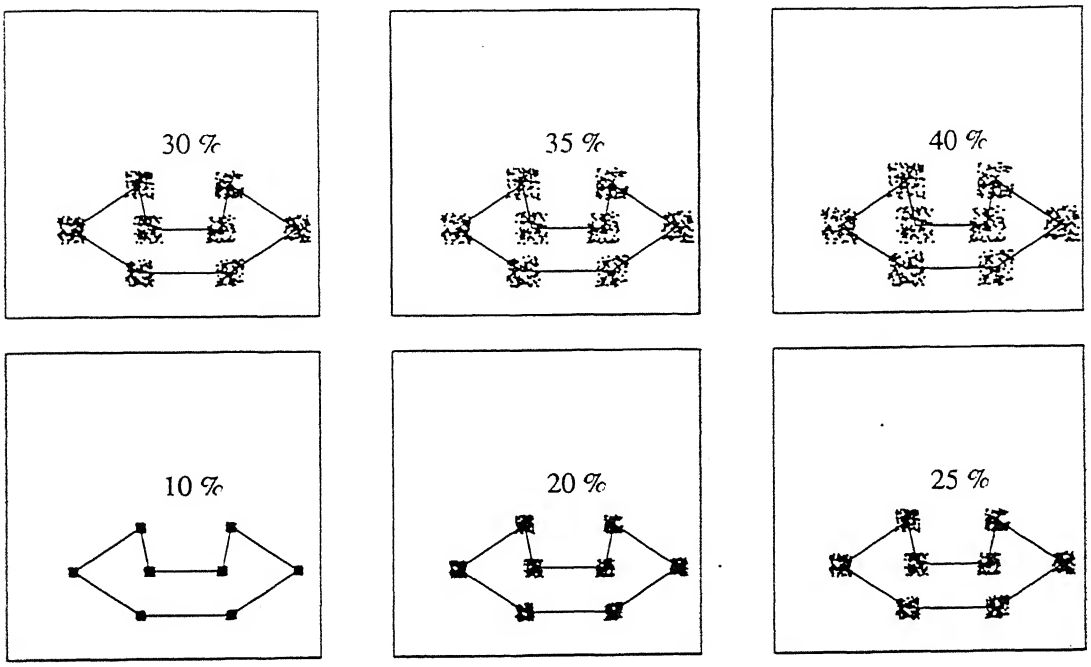

Figure 3.2: *Vertex Position Uncertainty.* Polygons are constructed between vertices within the scatter-plots shown. Each figure is labeled with the maximum dislocation in the vertex position as a percentage of the smallest edge length. The smallest edge may vanish or self-intersect for uncertainties approaching 50%.

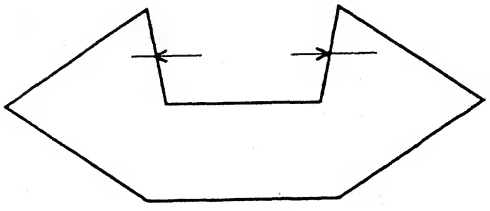

Figure 3.3: *Nominal Grasp.* Van-Duc Nguyen grasp points on the concave surface of the polygon of Figure 3.2.

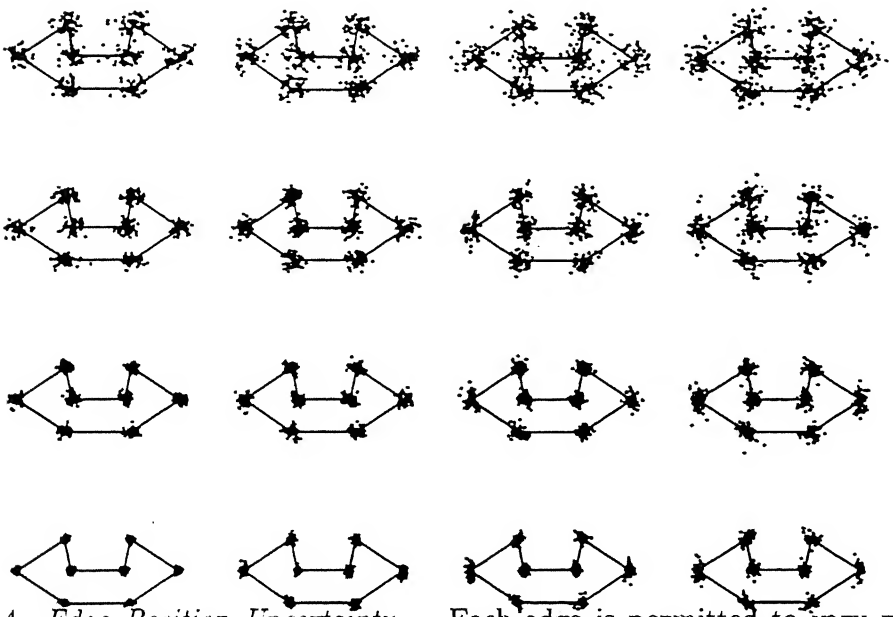

Figure 3.4: *Edge Position Uncertainty.* Each edge is permitted to vary with a given length and angle uncertainty. The resulting vertices are shown in a scatter plot. Horizontally, the Length uncertainty increases in each row (10%, 20%, 30% and 40% of the smallest edge). The Angle uncertainty increases vertically in fractions of $2\pi/100$, i.e. 0.2%, 0.5%, 0.75%, and 1% corresponding to 0.72, 1.8, 2.7, and 3.6 degrees respectively. In each case, a random set of edges is chosen in these zones and only nearly-closed shapes are retained. The robustness of the grasp for a set of 1600 such polygons is shown in Figure 3.13.

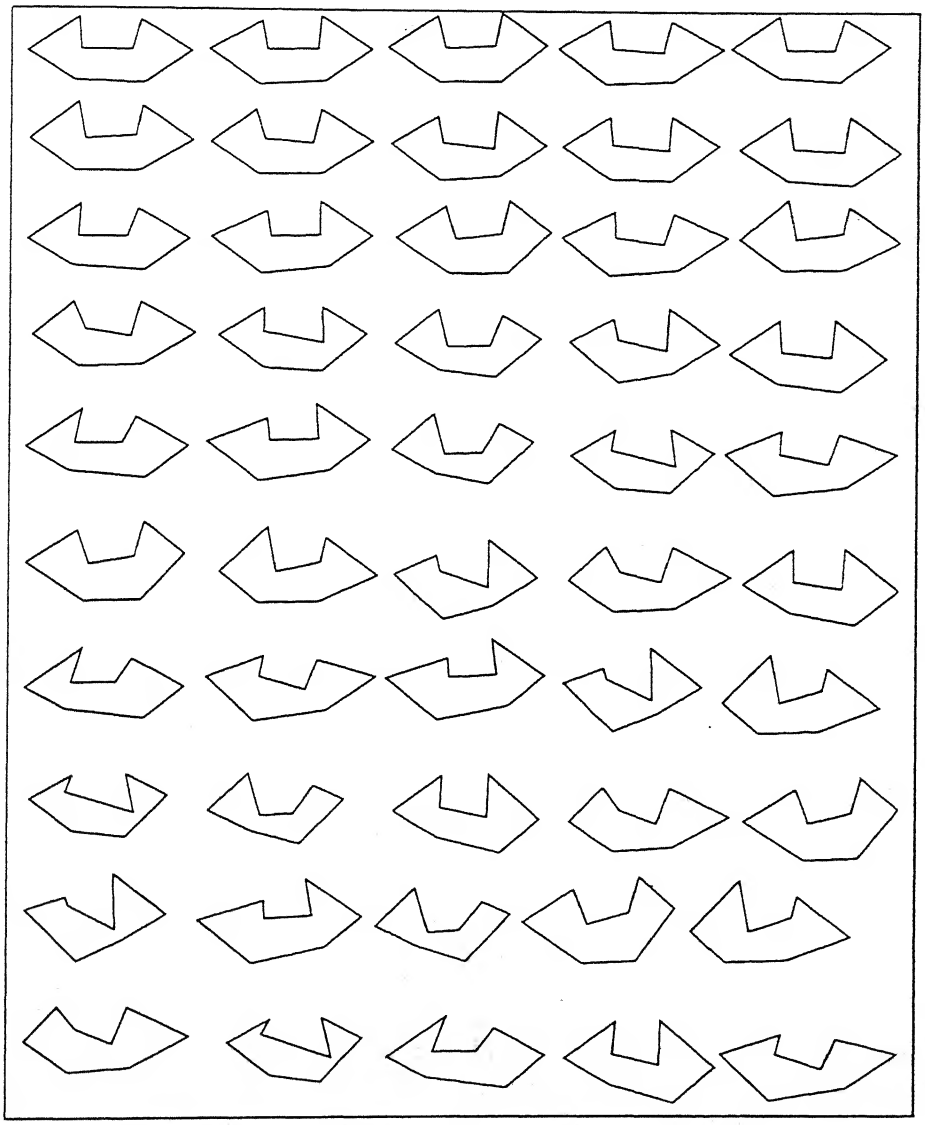

Figure 3.5: *Sample polygons - 8-sided* . These shapes are some 8-sided polygons generated within the uncertainty bounds for vertex position uncertainty cases (Figure 3.2). The top two rows show vertex uncertainty 10% and in the subsequent couples of rows the uncertainties are 20%, 30%,40% and 45% of the smallest edge length.

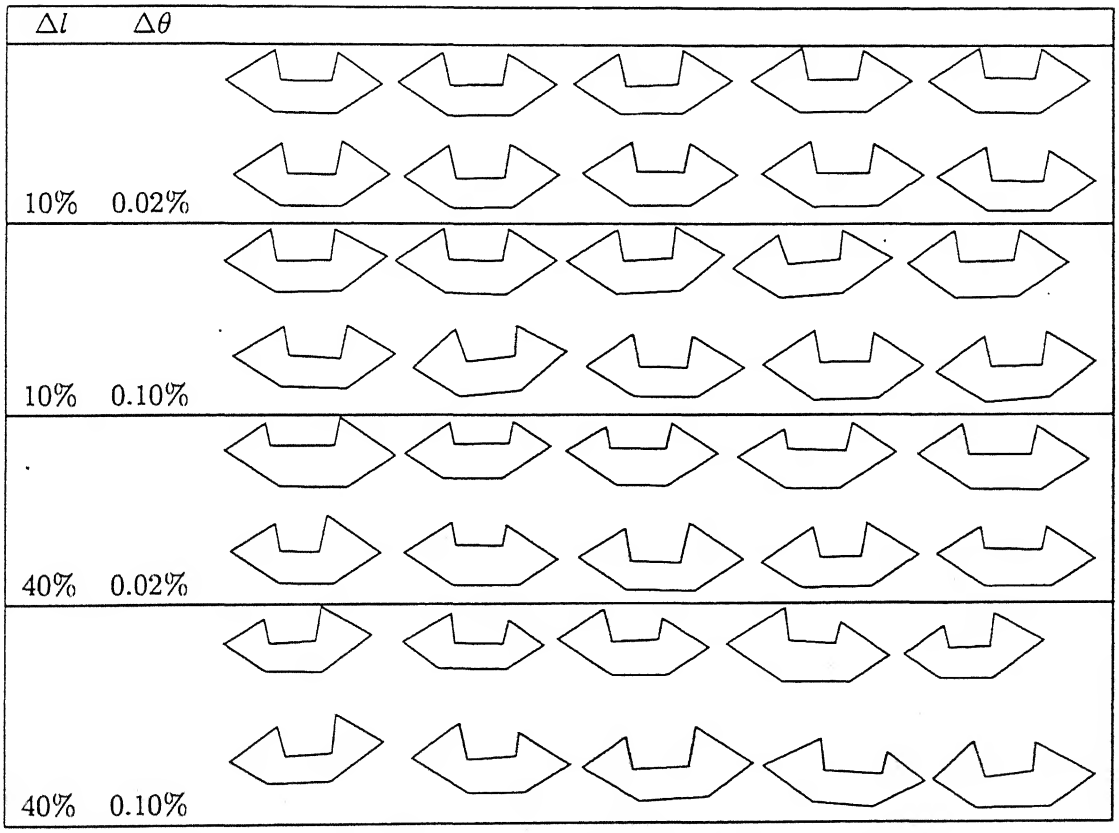

Figure 3.6: *Sample polygons - 8-sided* . These shapes are some 8-sided polygons generated within the uncertainty bounds for edge/length orientation uncertainty case. Where Δl is the unceratinty in edge lenth as percentage of samllest edge length and $\Delta\theta$ is uncertainty in adjacent angles as a fraction of 2π.

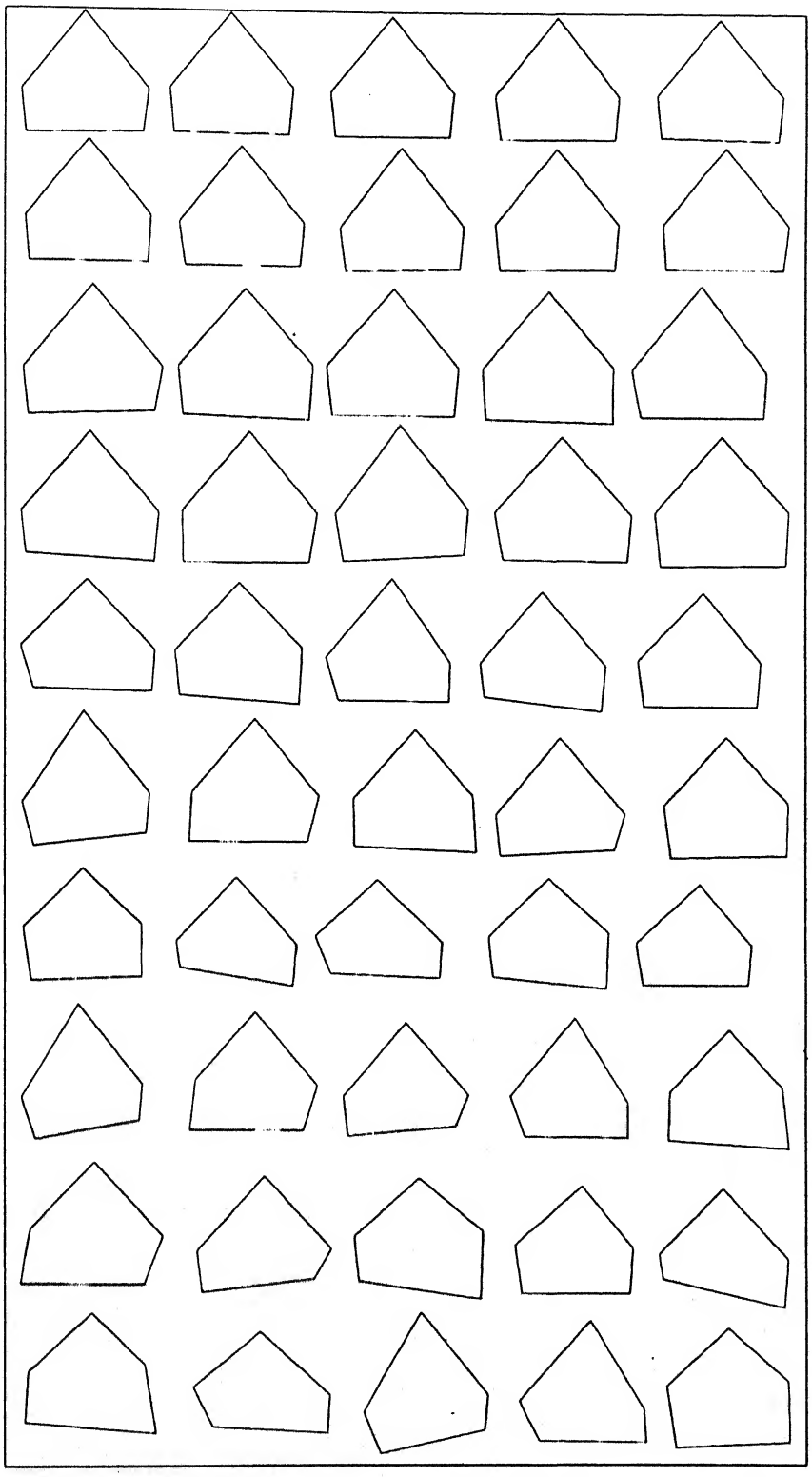

Figure 3.7: *Sample polygons - 5-sided* . These shapes are some 5-sided polygons generated within the uncertainty bounds for vertex position uncertainty cases. The first two rows show vertex uncertainty 10% and in the subsequent couples of rows the uncertainties are 20%, 30%,40% and 45% of the smallest edge length.

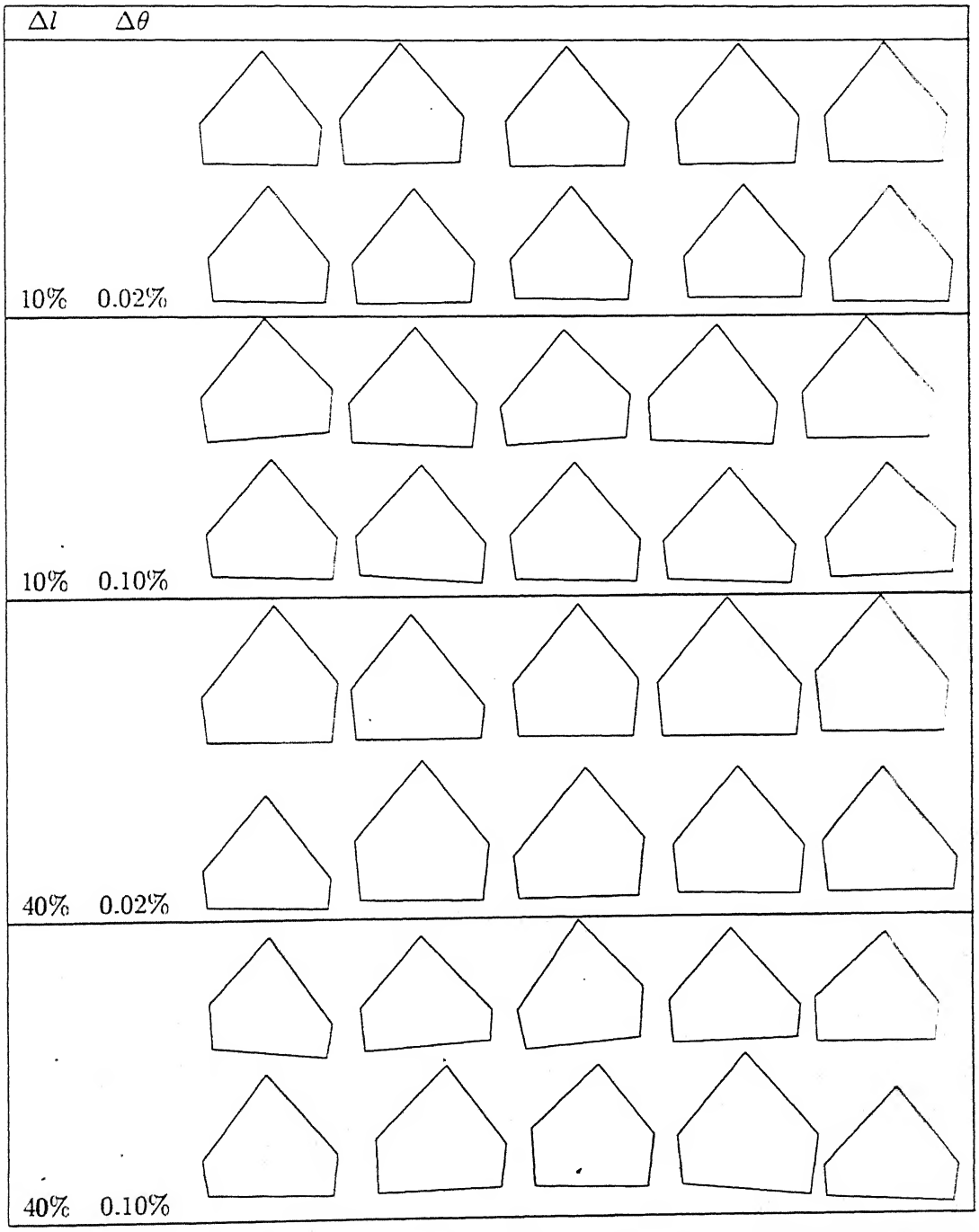

Figure 3.8: *Sample polygons - 5-sided* . These shapes are some 5-sided polygons generated within the uncertainty bounds for edge/length orientation uncertainty case. Where Δl is the unceratinty in edge length as percentage of samllest edge length and $\Delta\theta$ is uncertainty in adjacent angles as a fraction of 2π.

resulting in any of the following situations:

1. Those points may form a stable grasp.
2. Excessive Edge Angle: The points may be on two such edges that no stable grasp is possible on those edges i.e. the angle between two edges is more than 2ϕ (equation 2.6).
3. Position of the points: These points may be such that although a stable grasp is possible on those edges, these particular points do not form a pair of stable grasp. (equation 2.5).
4. Grasp points may migrate to some other edge.

3.3 Analytical Determination of failure due to excessive edge angle

Before embarking on an empirical study it is important to determine if a theoretical analysis is possible and under what approximations. As discussed in the previous section one of the reasons for grasp failure is that the angle between the grasp edges is such that there is no possible grasp on those edges. The following analysis illustrates the difficulty of a theoretical treatment for this problem. The probability of failure due to this reason in an uncertain grasp situation can be calculated to some extent analytically. Assuming that the vertex uncertainty is significantly less than the edge length, we present an analysis for both the Vertex Position Uncertainty Model and Edge Length/Orientation Uncertainty Model.

Consider an edge of length L at an angle θ, where vertices are uncertain by $(\pm\Delta X, \pm\Delta Y)$. Without loss of generality, we can assume its start point to be the origin and the end point to be the $X_e = (X_2 - X_1)$ and $Y_e = (Y_2 - Y_1)$ with twice the uncertainty $(\pm 2\Delta X, \pm 2\Delta Y)$. If $\delta\theta$ is the perturbed angle due to a vertex perturbation $(\delta X, \delta Y)$ then the slope variation $\delta(\tan\theta)$ is given by

$$\delta(\tan\theta) = \frac{Y_e + \delta Y}{X_e + \delta X} - \frac{Y_e}{X_e} = \sec^2\theta\delta\theta \tag{3.1}$$

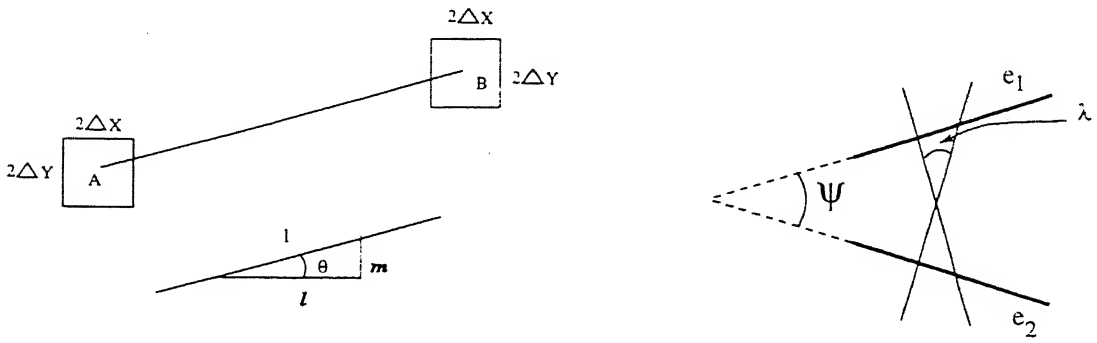

Figure 3.9: *An edge under Vertex Position Uncertainty.*(a) Edge AB whose vertices are under uncertainty ΔX and ΔY in X and Y direction respectively. (b) Two grasp edges with an angle ψ between them and angle of friction cone is $\lambda = tan^{-1}\ \mu$ - $\frac{\psi}{2}$. The grasp will fail if ψ is $2\tan^{-1}\mu$ or more.

$$\delta\theta = \left(\frac{X_e}{L}\right)^2 \left[\frac{\delta Y X_e - \delta X Y_e}{X_e(X_e + \delta X)}\right] \tag{3.2}$$

The maximum and the minimum $\delta\theta$ in this range can be written as:

$$\delta\theta = \frac{2\Delta}{L^2}\left[\frac{(X_e \pm Y_e)X_e}{X_e \mp 2\Delta}\right] \tag{3.3}$$

Where we assume isotropic error $\Delta X = \Delta Y = \Delta$.

This gives the range over which the θ is spread. But orientation of edge **AB** is not distributed evenly between θ_{min} and θ_{max}. This range of orientation of edge **AB** can be divided in three segments by the four θs at the maximal points of the uncertainty region at **B** ($4\Delta X$ by $4\Delta Y$). The probability that edge **AB** will lie in a band around a particular orientation(θ) is proportional to the length of the intercept $\mathbf{P_1P_2}$ on the uncertainty rectangle by a ray projected from **A** at angle θ. The following expression holds for an edge angle between θ_2 and θ_3 in Figure 3.10(b).

$$l_{P_1P_2}(\theta) = \left[(4\Delta)^2 + (4\Delta\tan\theta)\right]^{\frac{1}{2}} \tag{3.4}$$

Similar expressions can be derived in the other two zones. Thus a probablistic distribution for angle θ of edge **AB** can be derived.

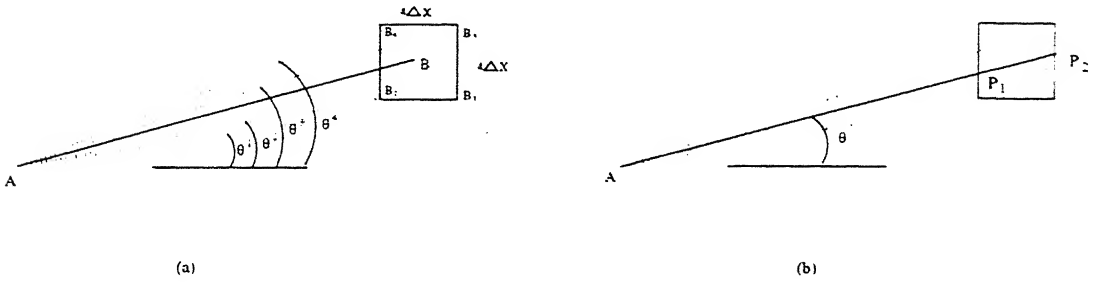

(a) (b)

Figure 3.10: (a) An edge **AB** which is having uncertainty of $\pm\Delta$ at both points can be replaced with an edge **AB** with one fixed point and other point having uncertainty $\pm 2\Delta$. (b) Getting a particular orientation θ will have a probability proportional to length of the intercept $\mathbf{P_1P_2}$ by a ray projected from point **A** at angle θ on the region of uncertainty around point **B**.

A grasp fails due to excessive edge angle only when the angle between the two grasp edges **AB** and **CD** exceeds $2\tan^{-1}\mu$. If the initial angle was ψ then the perturbed angle is $(\psi + \delta\theta_A B + \delta\theta_C D)$. Let the distribution function of $\theta_A B$ and $\theta_C D$ be given by expression $f_{\theta_{AB}}(\theta_A B)$ and $f_{\theta_{CD}}(\theta_C D)$ then the distribution function of the angle between **AB** and **CD** is given by.

$$g_\psi(\psi) = \int_{\theta_{AB}} \int_{\theta_{CD}} f_{\theta_{AB}}(\theta_{AB})\, f_{\theta_{CD}}(\theta_{CD})\, d\theta_{AB} d\theta_{CD} \tag{3.5}$$

This integral is extremely complex, and has nine cases corresponding to the three zones of θ, and will in any case need to be evaluated numerically. The failure due to position will entail even more complex analysis since it depends on the cumulative uncertainty of the intermediate edges as opposed to just the two edges here. These will require a numerical procedure whose cost is likely to be prohibitive compared to the Monte-Carlo simulation proposed below. Furthermore, if the shape uncertainty model changes (eg. vertex uncertainty zones are anisotropic, i.e. $\Delta x \neq \Delta Y$, or are elliptical as opposed to square) then the entire analysis will need to be reformulated. which is not the case in the simulation approach.

3.4 Methodology for Assessing Grasp Robustness

In this section we describe the methodology for assessing the robustness of the nominal grasp the simulation-based Monte-Carlo approach [14].

Algorithm For Finding Robustness of the Grasp Given a nominal polygon π_o, the bounds of the uncertainty (For vertex model $\Delta(x, y)$ or for edge based model $\Delta(\theta, l)$) and the direction of approach of grasp.

1. Find the grasp points for the nominal polygon (For this work we used the mid points of the maximal IROC computed on the basis of Van-Duc Nguyen algorithm).
2. Find a sufficiently large set $\{\pi_i\}$, of possible polygons in the given uncertainty bounds.(See Next Subsection)
3. For each π_i find the contact points for the given direction of approach of the robot fingers. These contact points are the points on the boundary of π_i where robot fingers will touch the polygon π_i approaching in the given direction towards the nominal grasp points.
4. Check for each π_i whether the corresponding contact point gives a stable grasp or not. The percentage of cases having stable grasp in the set $\{\pi_i\}$ gives the robustness of that nominal grasp for that direction of approach.

3.4.1 Size of set $\{ß_i\}$

Reliability of the Monte-Carlo method is critically dependent on the sample sizes. For this we performed the above mentioned test with sample sizes of 10, 20, 50, 75, 100, 250, 500, 1000, 10^4, and 10^5, and found that beyond about 1000, the percentage of failed cases remain unchanged as shown in Figure 3.11. This behaviour is true for several different random number seeding patterns. Based on this experiment, a sample size between 1000 to 1600 polygons was used in the following tests.

As discussed earlier in Section 3.2 we divided the grasp failure in two categories -

1. *Edge Angle:* Edge orientation may change such that there is no overlap between the friction cones for those two edges. These failure cases are labeled "Ang" in the Figure 3.11.

2. *Grasp Position:* Although the two edges can support successful grasps, the actual point obtained by the grasp trajectory do not provide a stable grasp (The line joining the contact points is outside the grasp convex, which is the intersection of the two friction cones on the two contact edges). This is labeled as "Pos" in the Figure 3.11.

The total failed cases are represented by label "Tot". As can be seen from the graph, for this type of polygon, the result is fairly stable after about 1000 sample. This behaviour is true for several different random number seeding patterns. Based on this experiment, 1000 to 1600 polygons were generated for each data point.

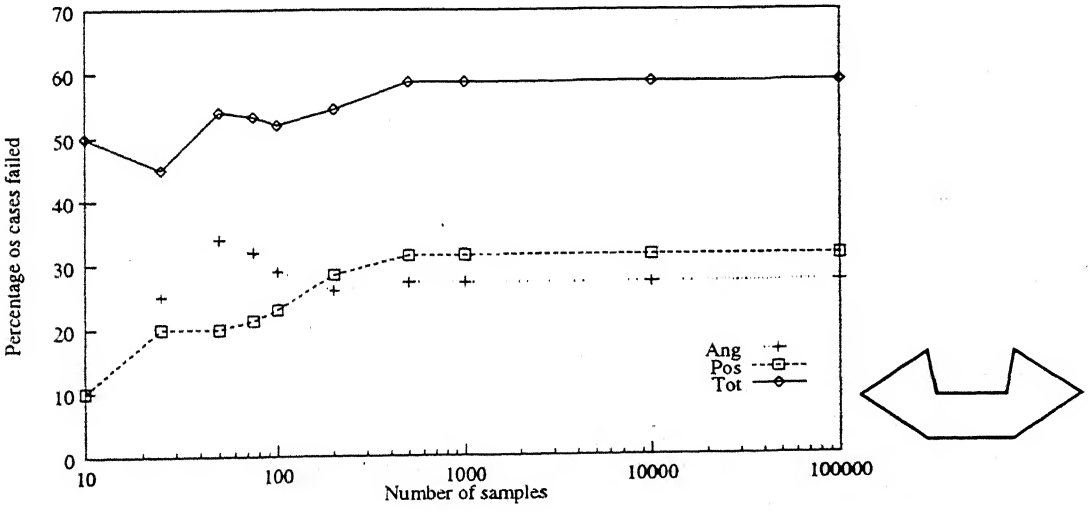

Figure 3.11: *How many polygons to test?* Empirical results are often subject to sample sizes. Tests were conducted with sample sizes of 10, 20, 50, 75, 100, 250, 500, 1000, 10^4, and 10^5, and show that beyond about 1000, the percentage of failed cases remain unchanged. This behaviour is true for several different random number seeding patterns. Based on this experiment, 1000 to 1600 polygons were generated for each data point.
In each of the following figures, the shape of the polygon is shown in the bottom left of the graphs. The results show the effect of increasing uncertainty on the percentage

of failed cases.

3.5 Shape Uncertainty Model

3.5.1 Edge Uncertainty Model

Here a polygon is defined in terms of each edge length, angles between two adjacent edges, position of one vertex of the polygon and orientation of one edge in respect to the work space frame. In this uncertainty model one thousand to sixteen hundred samples were generated from a given nominal polygon based on given uncertainty bounds of edge length and the angle between adjacent edges. For defining the orientation and position of the shape in the work space we are defining coordinates of one point and also orientation of one edge from that point. The uncertainty model may be biased towards the vertex whose position is defined and the edge whose orientation is defined, because uncertainty bounds are only for edge length and the angle between adjacent edges. To overcome this bias we generated an equal number of bounded polygons taking each vertex as the first vertex of that chain code.

3.5.2 Vertex Uncertainty Model

In this model also one thousand to sixteen hundred polygons were generated in the given uncertainty shape class. The vertex uncertainty was defined as a fraction of the smallest edge length (2% to 50% of the smallest edge length). We assumed that in a vertex based model where the position of the vertices was used to define the polygon the certainty in the vertex position is related to the accuracy by which two vertices can be distinguished (or the smallest edge length).

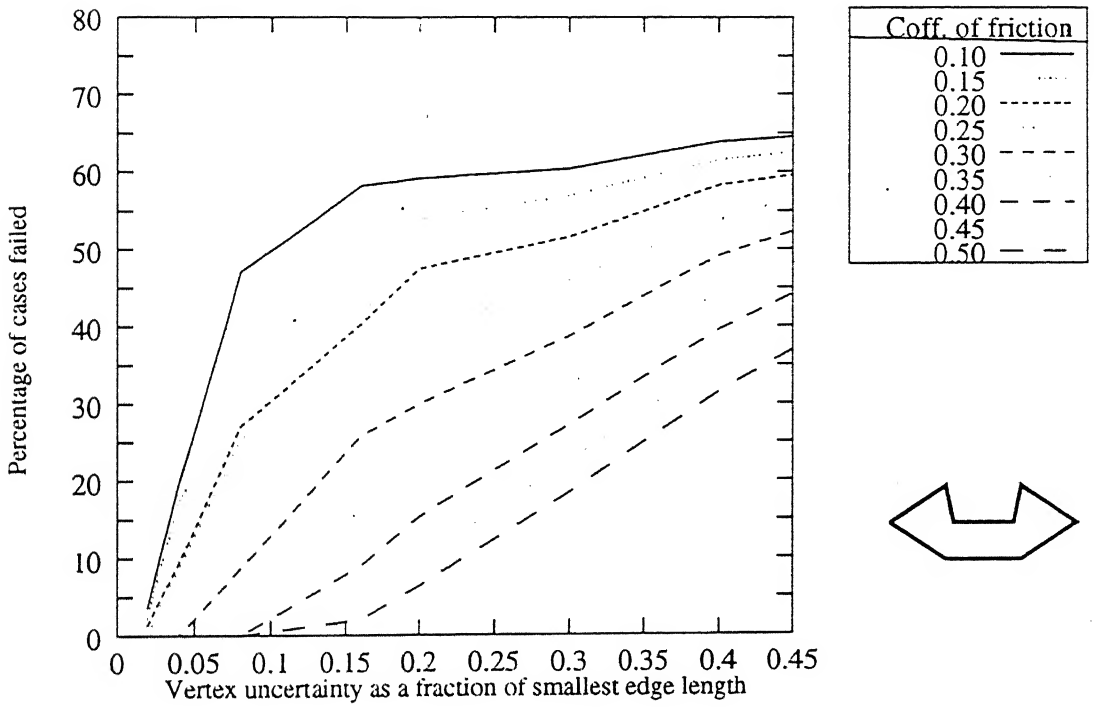

Figure 3.12: *Effects of Coefficient of Friction; Vertex Uncertainty Model* As friction increases, the grasp convex broadens and the percentage of failure for any given uncertainty is less. When friction is high, small uncertainties have little effect, whereas for very low friction, even the smallest uncertainty causes a high failure rate.

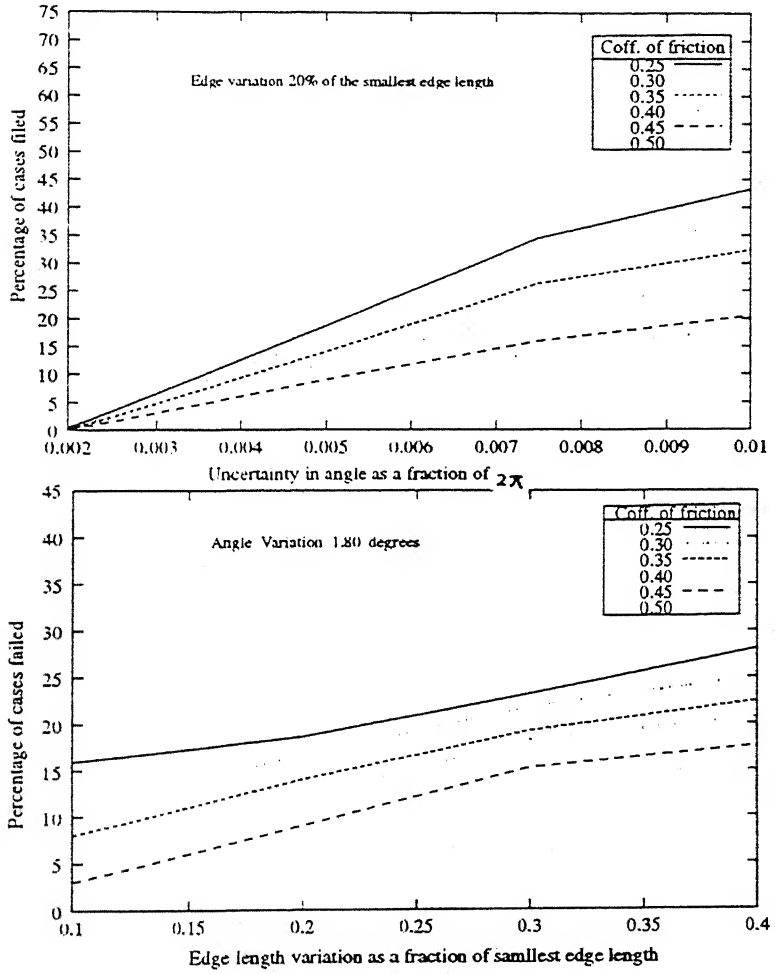

Figure 3.13: *Effects of Coefficient of Friction: Edge Uncertainty Model.* Edge uncertainty may be in angle or in edge-length. Small angular variations have a small effect at any coefficient of friction, whereas for edge-length variations, the effect of friction is more pronounced. This is because when the edge angles are not allowed to vary much, the uncertain shapes are almost the same as the nominal polygon, and the nominal grasp has a higher probability of being effective. Changing edge-lengths may cause global changes in the shape. Each data point reflects 1600 samples.

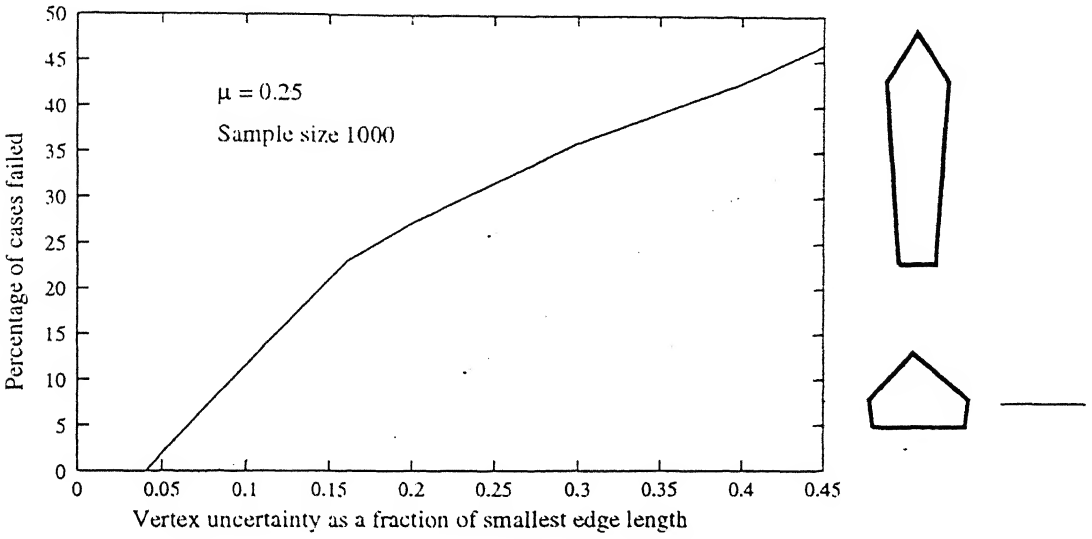

Figure 3.14: *Effects of Shape: Long vs. Short aspect ratios.* In the short aspect ratio case, small shape uncertainty can result in relatively higher edge dislocation, causing the nominal grasp to fail. This analysis uses the vertex uncertainty model.

3.6 Simulation Results

In this section we discuss the results obtained by the Monte-Carlo simulation of grasp robustness based on errors in the shape of the different polygons. In most of the cases results are monotonic. i.e. as the uncertainty increases, robustness decreases or as the coefficient of friction increases robustness increases. The exception to this is discussed in the section 3.7.3.

3.6.1 Effect of friction

In a force-closure grasp, coefficient of friction plays an important role in deciding the stability of a grasp. In actual situation the of coefficient friction may not be known exactly, and this is also a source of grasp uncertainty. For this reason we have simulated these results over a wide range of friction values, from 0.1 to 0.5. When μ is greater than 0.3, and vertex uncertainty is less than 1%, there are no failure cases at all (Figure 3.12). In edge length/orientation uncertainty model small angular variations have little effect on robustness at any coefficient of friction because when

the angles are not allowed to vary much, the perturbed shapes retain approximately the same shape even if the edge length has high variability (Figure 3.13.

3.6.2 Effect of Aspect Ratios

In polygons of short aspect ratio the effect of shape uncertainty is more pronounced than in objects of higher aspect ratio, because the uncertainty in position of vertex is defined in terms of the smallest edge length so the longer edges retain their angle in perturbed shapes, in comparison to polygons of small aspect ratio. More over chances that a different edge will be encountered by the fingers trajectory is less in higher aspect ratio polygons (Figure 3.14).

3.6.3 Anomalous effects when grasp not feasible

With some shapes there was no feasible grasp on the nominal shape for a low coefficient of friction. In such cases the nominal grasp calculated for average value of coefficient of friction was initially infeasible for that low coefficient of friction. But as the uncertainty increases percentage of successful grasps seems to increase since some of the perturbed shapes now provide a valid grasp. In Figure 3.15 to Figure 3.19 we observe the anomalous effect as a curve in the upper portion of the graph. There the failure percentage starts starts from 100 and comes down (even up to 80% in some cases) as the uncertainty is increased.

3.6.4 Tests on random shapes

To test this grasp robustness methodology over a range of polygons we tested it on some random polygonal shapes. Results were of same type as for regular polygons because the methodology is not directed towards any particular type of polygon (Figure 3.15, Figure 3.16, Figure 3.17). In each case the input nominal shape was generated and the best initial grasp found, then 1600 perturbed shapes were generated at each uncertainty level and tested under different coefficients of friction. etc.

The random polygons used were generated by a random polygon generator based on chain code uncertainty model. An 8-sided regular polygon was input and the uncertainty bound of the edge length was set equal to it self (edge can vary from zero to double of the original edge length) and orientation uncertainty equal to 2π. The polygon generated within these bounds are quite random to each other and not biased to the input polygon at all as it is quite clear in Figure 3.20. In fact, this random polygon generator may be better than many other, but since this was not the main thrust of the work, this point was not pursued further.

Besides this Kamon et.al [7] in their work have used some generalized cone shapes for testing a system which learns to grasps the object by analyzing the visual information gathered by vision. These shapes are axially symmetric, we tested this methodology on some such samples also (Figure 3.18.Figure 3.19). Since they do not consider shape variations, our results cannot be compared.

3.7 Experimental Validation

Simple experiments were conducted on a five-sided convex shape to test for the effects of uncertainty. The nominal grasp is determined on a model that is different from the actual sample used, the difference being a percentage of the uncertainty being tested for. The two fingers are now moved as if to grasp this nominal object, and halted at the point of contact. The experiment has the drawback that the results depend on the coefficient of friction, which could not be estimated very accurately in this case. The test was to physically try to dislodge the grasped object.

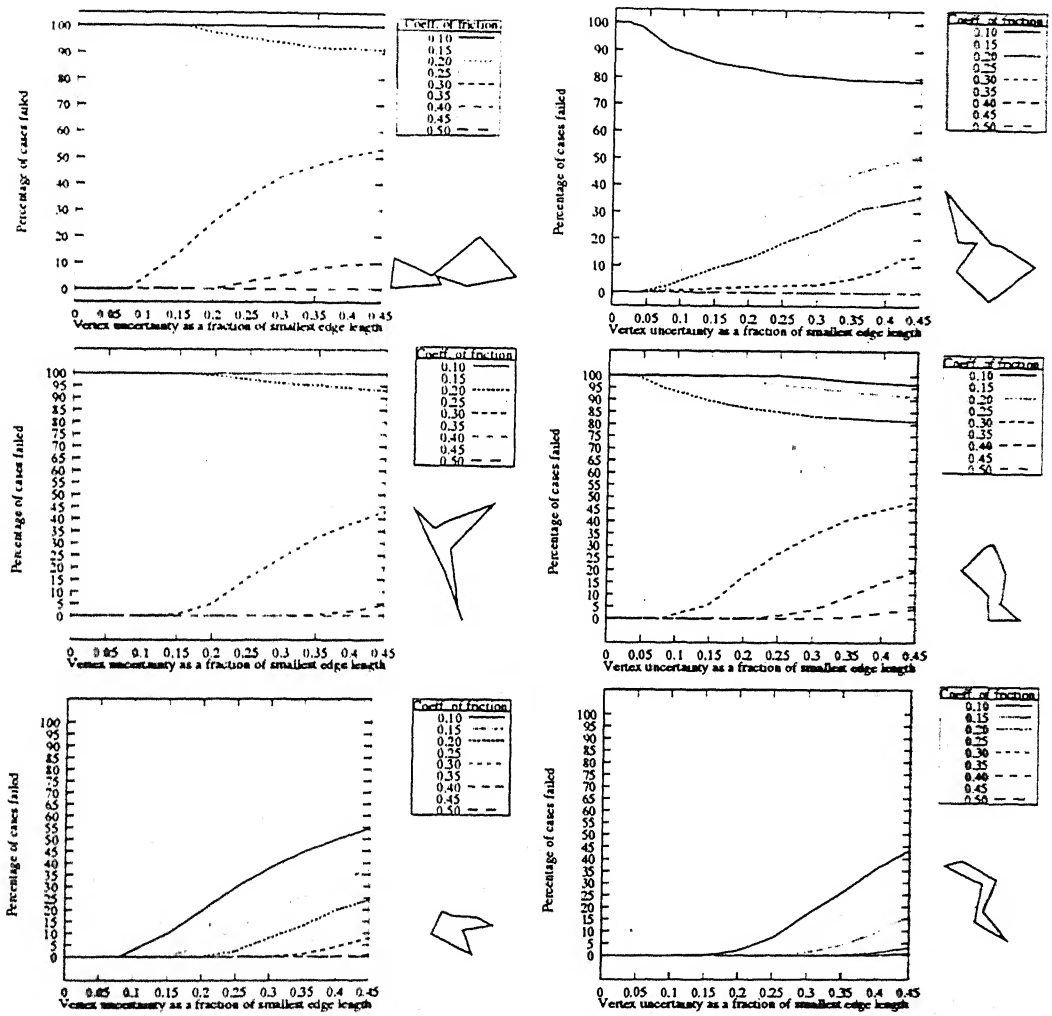

Figure 3.15: *Vertex position Uncertainty results for random polygons:* These graphs shows the change in robustness of the nominal grasp for six random polygons. Results are of the same type as for the previous polygons

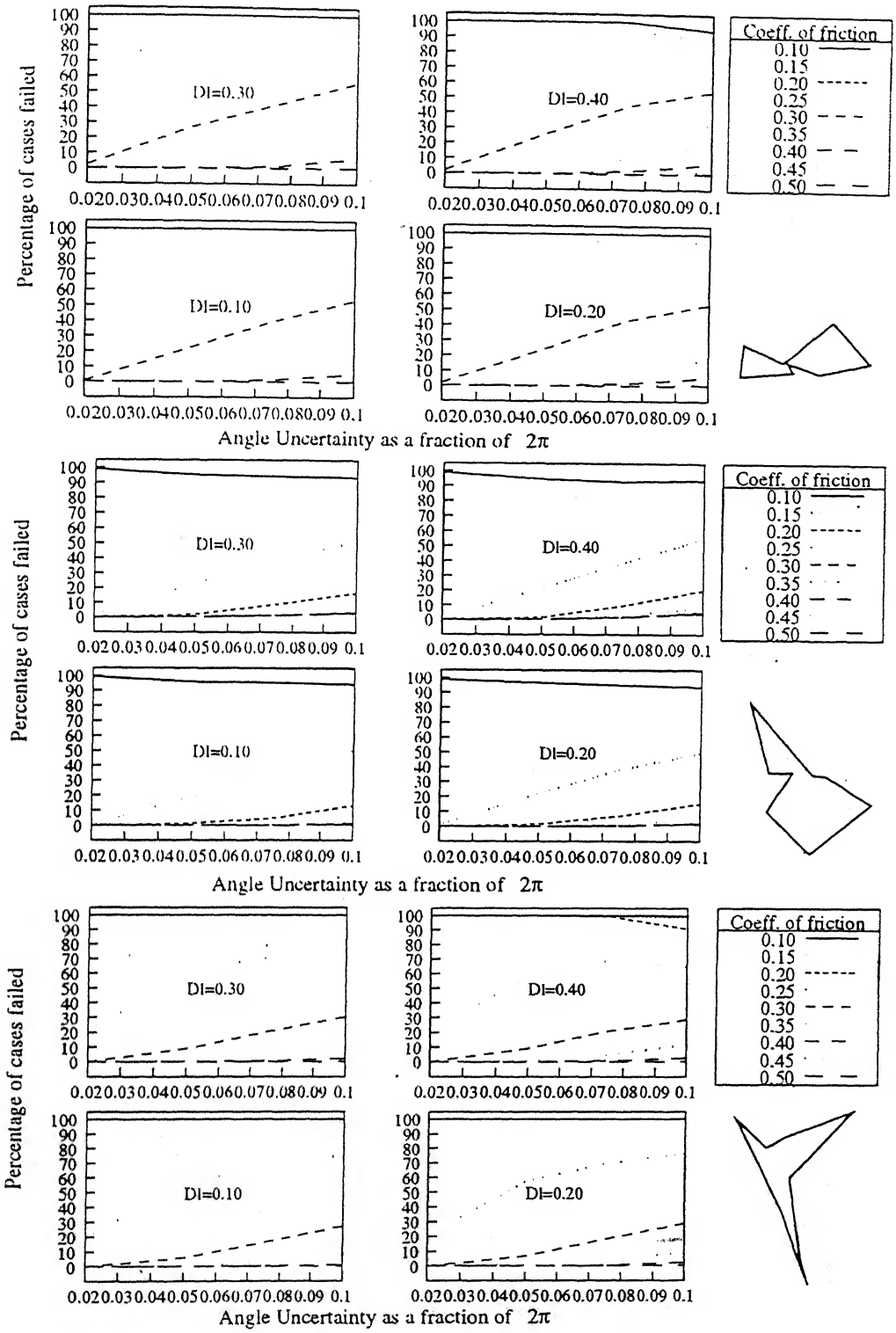

Figure 3.16: *Edge length/orientation Uncertainty:* These graphs show the variation of the grasp robustness for the first three random polygons from Figure 3.20

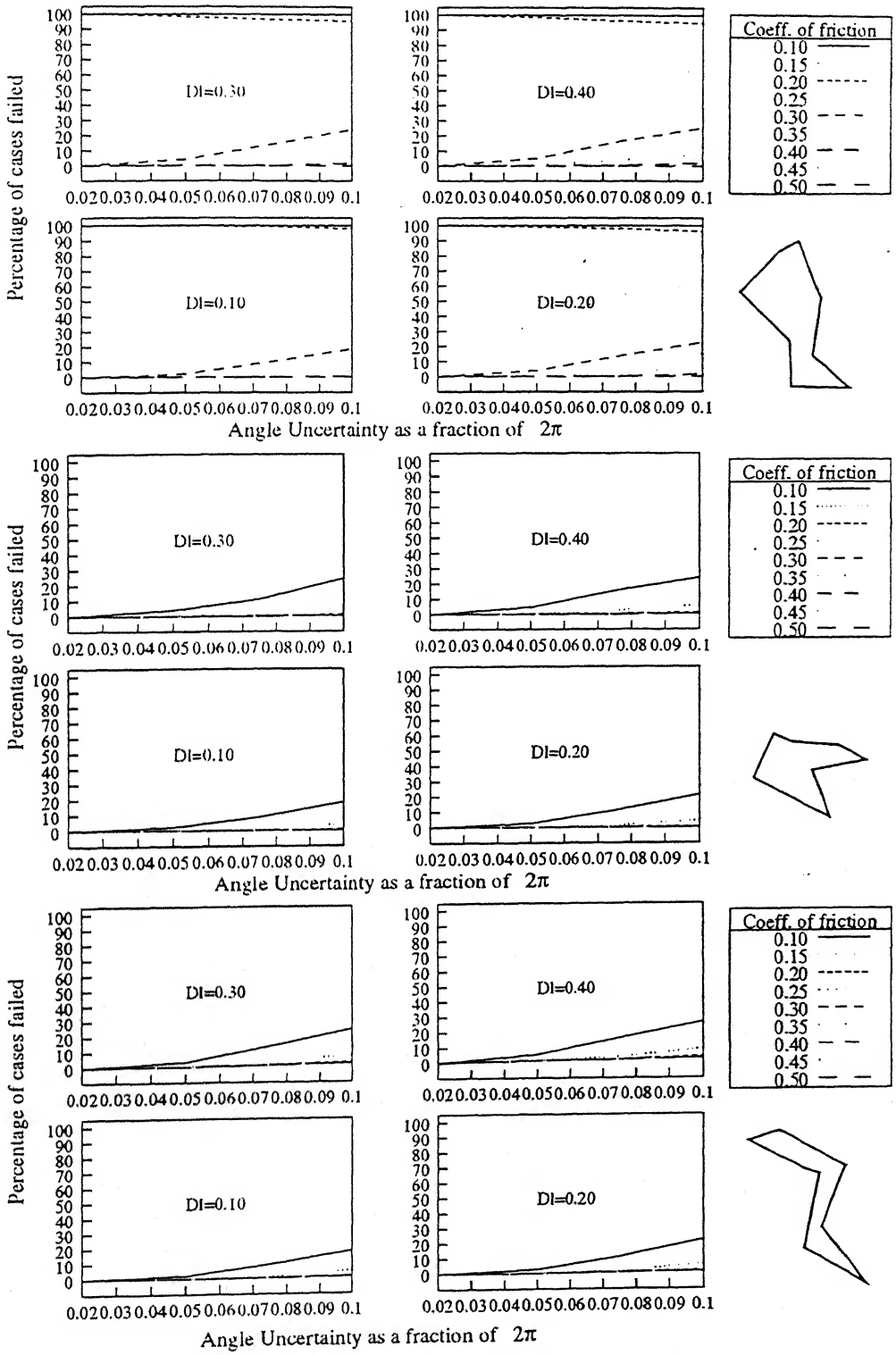

Figure 3.17: *Edge length/orientation Uncertainty:* Thes graphs shows the variation of the grasp robustness for another three random polygons from Figure 3.20

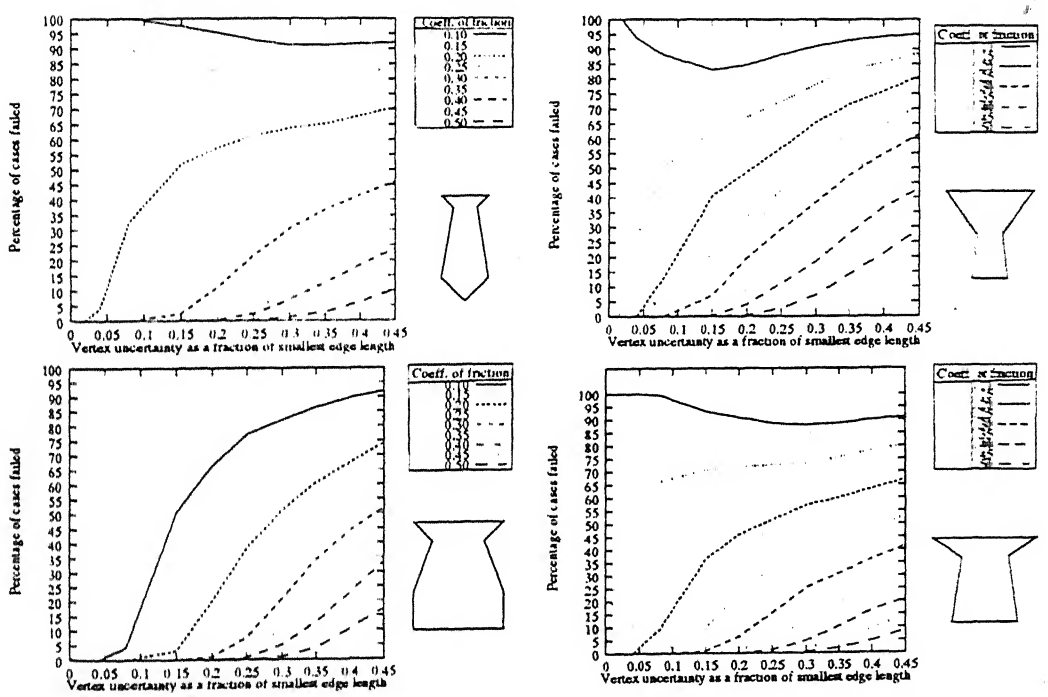

Figure 3.18: *Generalized Cones Vertex Position Uncertainty:* These graphs show the test on Generalized Cones [7] for vertex position uncertainty model

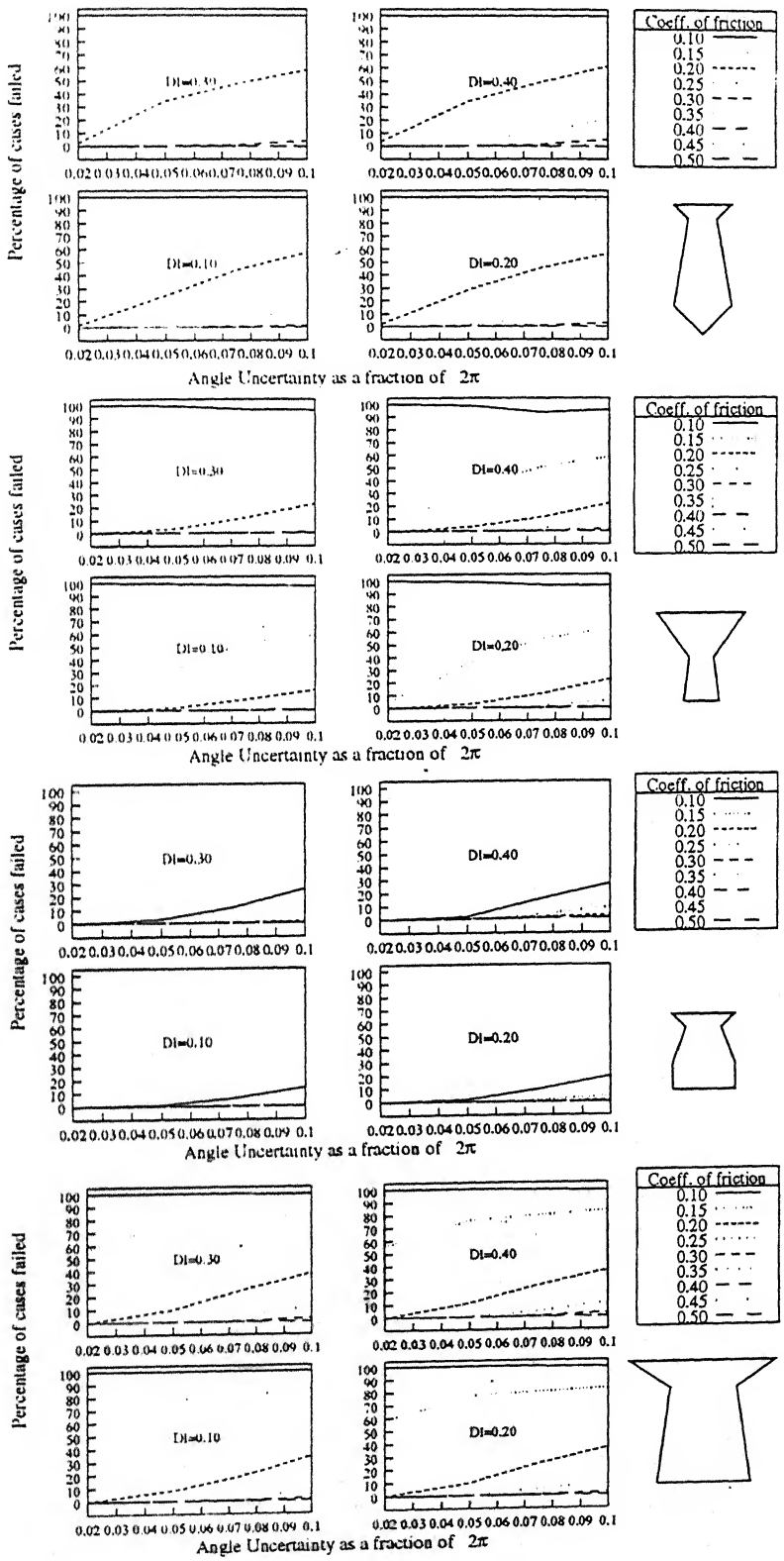

Figure 3.19: *Generalized Cones Edge Uncertainty:* These graphs show the test on Generalized Cones [7] for edge length/orientation uncertainty model

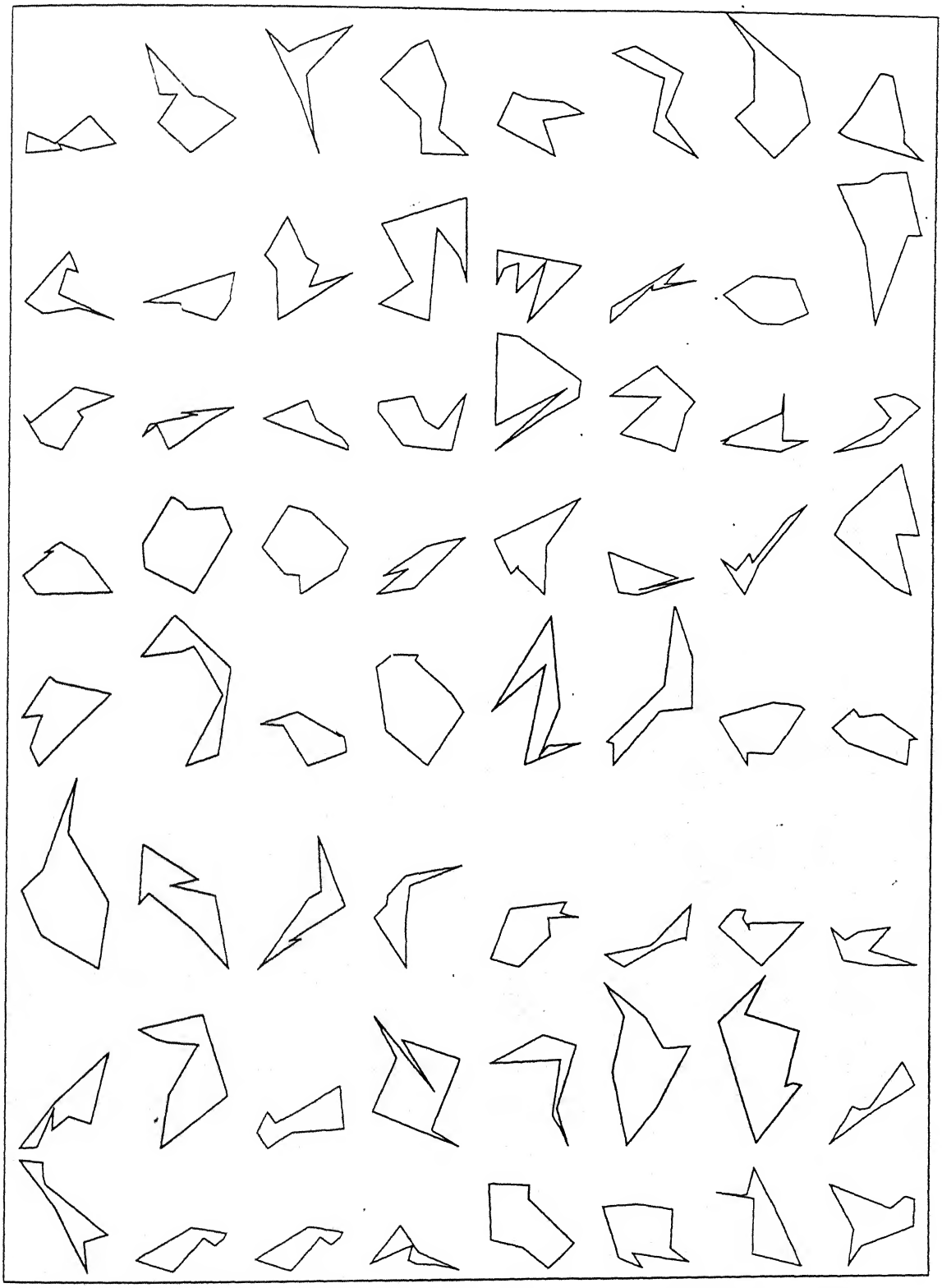

Figure 3.20: *Random polygons:* First six polygons of this lot of random polygons were used to verify the methodolgy proposed.

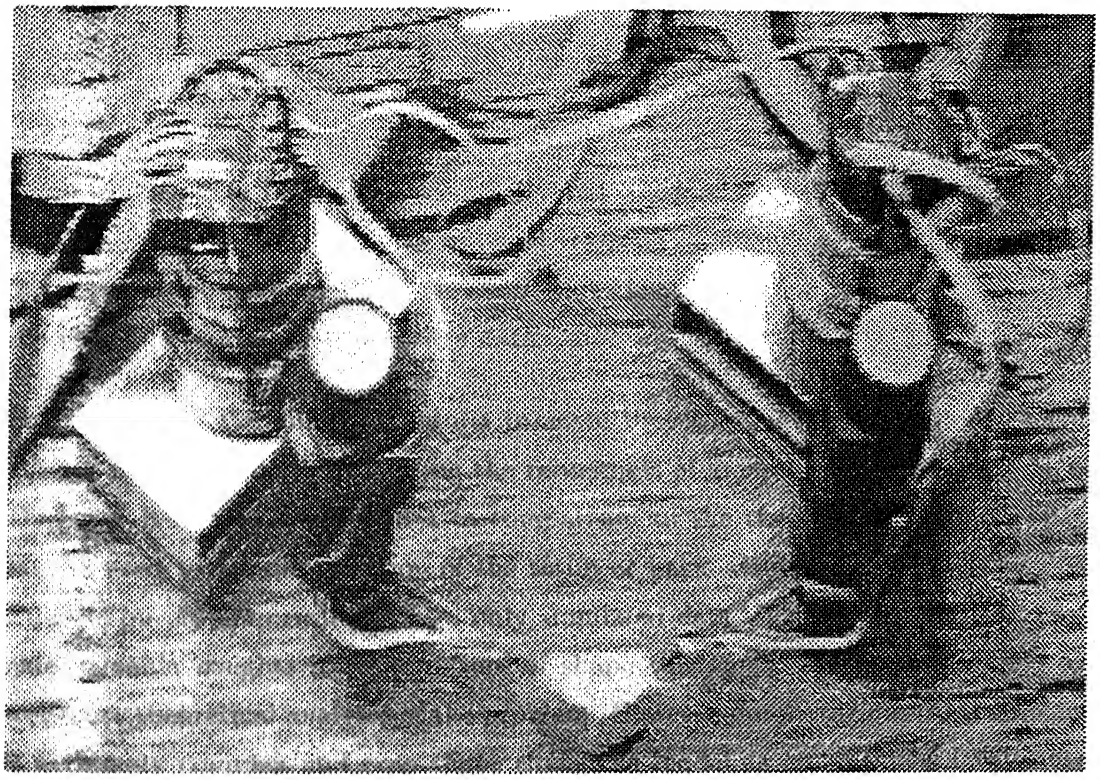

Figure 3.21: *The experimental Setup.* Each robot finger is a two degree of freedom planar manipulator. The second link is instrumented to detect contact forces (not used in this experiment).

Chapter 4

Conclusions

4.1 Conclusion

Given an object to be grasped, the model that is passed to the robot may differ from the actual due to different types of errors, causing different variations in the shape. In this work we have analyzed the shape variation errors that arise due to errors in the vertex positions, or in the edge data.

Based on this, the empirical results indicate that the methodology adopted provides a strong basis for estimating the robustness of grasp based on nominal data. Moreover it is very flexible idea in comparison to the theoretical treatment, and can be used to handle variation of the setup or basic assumptions. Therefore this study is purely empirical and uses only simulated data. The results obtained provide valuable insights into the nature of shape variations, which may be used to construct theoretical analyses of the problem. However purely theoretical treatment is extremely complex and even slight change in modeling assumptions invalidates the method. Results from such theoretical analysis for shape uncertainty even when available, need to be validated against empirical results.

The greatest difficulty of testing empirically is the modeling of shape variations. These variations must result in shapes that are valid, and yet within some neighbourhood of the initial shape.

Only two models of shape uncertainty have been modeled here. Another extension of this work would be to attempt to model other shape uncertainties that arise due to cognitive notions of shape as in medial axis models [9] or in mobile robot sensing as in grid occupancy models [8]. In addition to these aspects in robotics, our informal queries during this work revealed the scarcity of mechanisms for generating random polygons. As demonstrated in Figure 3.20, the approach of using the edge length/orientation uncertainty model with very wide ranges of variations results in a very widely varied sets. While we have not compared this approach to other methods for generating random polygons, this method also holds considerable promise as a random polygon generator.

In addition to grasping, effects of such shape uncertainty need to be investigated in motion planning, computer vision, other sensing modalities, linguistic task description, etc. Thus the shape uncertainty models developed here are likely to find application in a wide variety of problems.

Bibliography

[1] Brost, R.C.: 1988. Automatic Grasp Planning in the Presence of Uncertainty, *The International Journal of Robotics Research*, February 1988, v.7(1):p.3-17.

[2] Cohn, A.G.: 1995. A Hierarchical Representation of Qualitative Shape based on Connection and Convexity, *International Conference on Spatial Information Theory COSIT-95*. Semmering (Austria) September 21-23. 1995, [ftp://agora.leeds.ac.uk/scs/doc/srg/COSIT95.ps.gz]

[3] Desai, Rajiv. Jing Xiao and Richard A.Volz; 1988. Contact formations and design constraints: A new basis for the automatic generation of robot programs, *Robotica*, 1988.v.3:p.361-395

[4] Donald, Bruce: 1986. Robot motion planning with uncertainty in the geometric models of the robot and the environment: a formal framework for error detection and recovery. *IEEE International Conference on Robotics and Automation*, San Francisco, April 7-10. 1986,v.2:p.1588-1593.

[5] Ronald S. Fearing; 1986. Simplified Grasping and Manipulation with Dextrous Rob Hands. *IEEE Journal of Robotics and Automation*, December 1986,v.2(4) p.23-30.

[6] Fua, P. and A. J. Hanson: 1987. Resegmentation Using Generic Shape: Locating General Cultural Objects. *Pattern Recognition Letters*, March 1987, v.5(3):243-247.

[7] Ishay Kamon. Tamar Flash and S. Edelman; 1996 Learning to Grasp Using Visual Information *IEEE International Conference on Robotics and Automation*, Minnesota April. 1996. v.7(3):p.2470-2476.

[8] Moravec, Hans P.: 1987 Sensor Fusion in Certainty Grids for Mobile Robots, *Sensor Devices and Systems for Robotics*, ed. Alicia Casals, Springer-Verlag, p.253-276.

[9] Mukerjee, Amitabha: N. Tiwari; N. Hussain; and R. Agarwal; 1997 Ambiguous Shape Modeling using Axis models, *Journal of Artificial Intelligence in Engineering Design*, and Manufacture, (AI-EDAM), 1997, v.11(4).

[10] Van-Duc Nguyen: 1988. Constructing Force-Closure Grasps, *The International Journal of Robotics Research*, 1988, v.7(3), p.3-16.

[11] Van-Duc Nguyen; 1986. The Synthesis of Stable Force-Closure Grasps, *MIT Artificial Intelligence Laboratory*, Technical Report AI-TR/905, July 1986.

[12] Requicha, A.A.G.; 1980 Representation of Rigid Solid Objects *Computer-Aided Design*, ed. J. Encarnacao. Springer-Verlag, 1980, p.3-77.

[13] Schlieder, Christoph, 1994. Qualitative shape representation In*Spatial conceptual models for geographic objects with undetermined boundaries,* ed. A. Frank, London: Taylor and Francis.

[14] I. M. Sobol, 1984. The Monte-Carlo Method and Simulation, ed. Mir. Publishers, Moscow.